Ratiometric Luminescent Sensing of Biomarker for Sugar Consumption in Aqueous Medium by Cu(II)Coordination Polymer

Somnath[a], Musheer Ahmad[b] and Kafeel Ahmad Siddiqui[a]

[a]Department of Chemistry, National Institute of Technology Raipur, G E Road Raipur – 492010, Chhattisgarh, India

[b]Department of Applied Chemistry, Faculty of Engineering and Technology, ZHCET, Aligarh Muslim University, Aligarh, UP (India) – 202002

[a] e-mail: kasiddiqui.chy@nitrr.ac.in

Table S1 Crystallographic and structural refinement parameters for $[Cu(Hadp)_2(Bimb)]_n$ (**KA@CP-S3**).

Empirical formula	$C_{26}H_{32}CuN_4O_8$
Formula weight	592.11
Temperature/K	293(2)
Crystal system	Triclinic
Space group	$P\bar{1}$
a/Å	8.4173(5)
b/Å	8.4366(5)
c/Å	10.5472(7)
α/°	92.125(5)
β/°	93.821(6)
γ/°	118.349(6)
Volume/Å^3	655.69(8)
Z	1
ρ_{calc}g/cm^3	1.4994
μ/mm^{-1}	0.890
F(000)	309.5
Crystal size/mm^3	0.47 × 0.27 × 0.14
Radiation	Mo Kα (λ = 0.71073)
2θ range for data collection/°	3.88 to 51
Index ranges	$-10 \le h \le 10$, $-10 \le k \le 10$, $-13 \le l \le 13$
Reflections collected	15059

Independent reflections	2447 [R_{int} = 0.0922, R_{sigma} = 0.0611]
Data/restraints/parameters	2447/0/179
Goodness-of-fit on F^2	1.042
Final R indexes [I>=2σ (I)]	R_1 = 0.1362, wR_2 = 0.4106
Final R indexes [all data]	R_1 = 0.1501, wR_2 = 0.4186
Largest diff. peak/hole / e $Å^{-3}$	2.95/-1.13
CCDC No.	2233819

Table S2 Selected bond lengths [Å] and bond angles [°] for $[Cu(Hadp)_2(Bimb)]_n$ (**KA@CP-S3**).

[Cu(Hadp)$_2$(Bimb)]$_n$ (KA@CP-S3)					
Bond lengths [Å]					
Cu1–O1	1.968(9)	Cu1–O3	2.735	Cu1–N1	1.981(11)
Cu1–O1^1	1.968(9)	Cu1–O3^1	2.735	Cu1–N1^1	1.981(11)
Bond angles [°]					
O1^1–Cu1–O1	180.0	N1^1–Cu1–O3	89.8	N1–Cu1–O1^1	89.2(4)
N1^1–Cu1–O1^1	90.8(4)	N1–Cu1–O3	90.2	N1–Cu1–O1	90.8(4)
N1^1–Cu1–O1	89.2(4)	O3–Cu1–O3^1	180.0	N1^1–Cu1–N1	180.0
O1^1–Cu1–O3	94.9	O3^1–Cu1–N1^1	90.2	O1^1–Cu1–O3^1	85.1
O1–Cu1–O3	85.1	O3^1–Cu1–N1	89.8	O1–Cu1–O3^1	94.9

Symmetry codes for **KA@CP-S3**: (i) 1-X,2-Y,1-Z; (ii) 1-X,1-Y,2-Z

Table S3 Chemical structures dyes included in present work.

Anionic Dyes	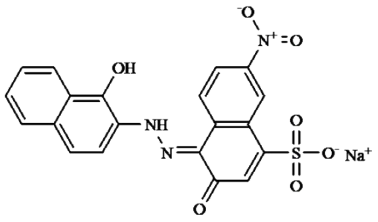 **(EBT)** 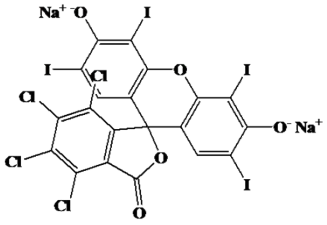 **(RB)** 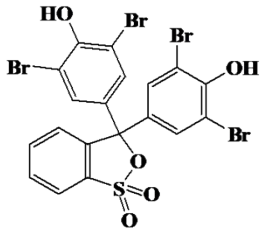 **(BPB)** 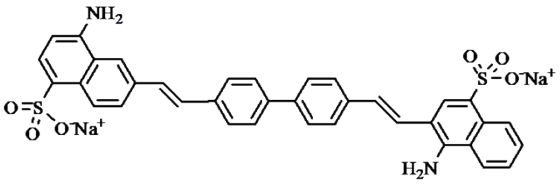 **(CR)** 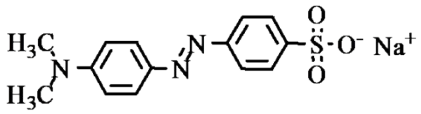 **(MO)**
Cationic Dyes	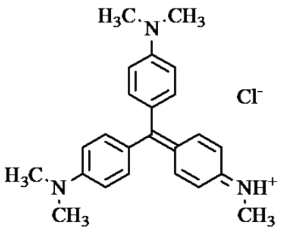 **(MV)** 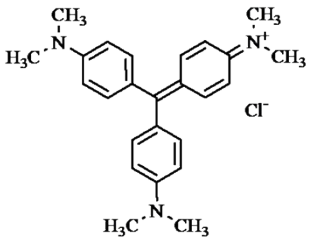 **(CV)** 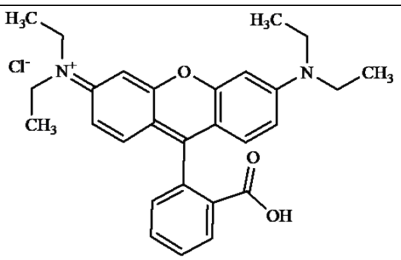 **(RhB)** 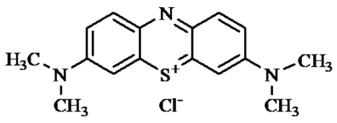 **(MB)** 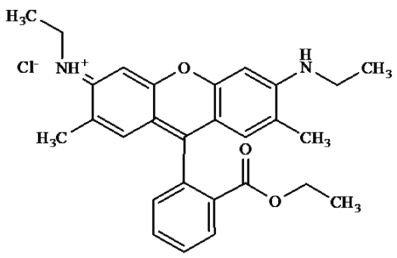 **(Rh6G)** 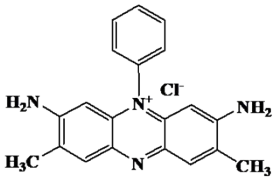 **(SO)**
Neutral Dyes	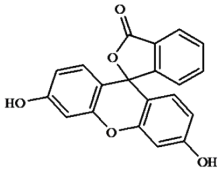 **(FS)** 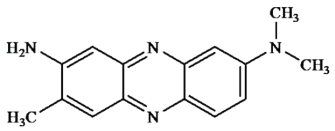 **(NR)**

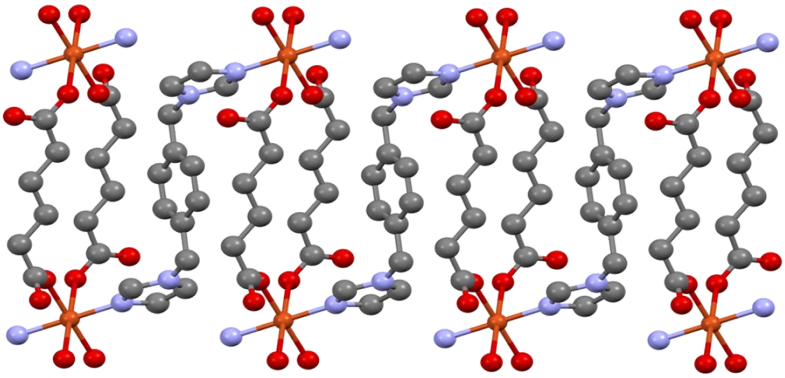

Fig. S1 View of 1D coordination polymer of **KA@CP-S3** formed through both $Hadp^{-}$ and Bimb ligands along crystallographic "a" axis.

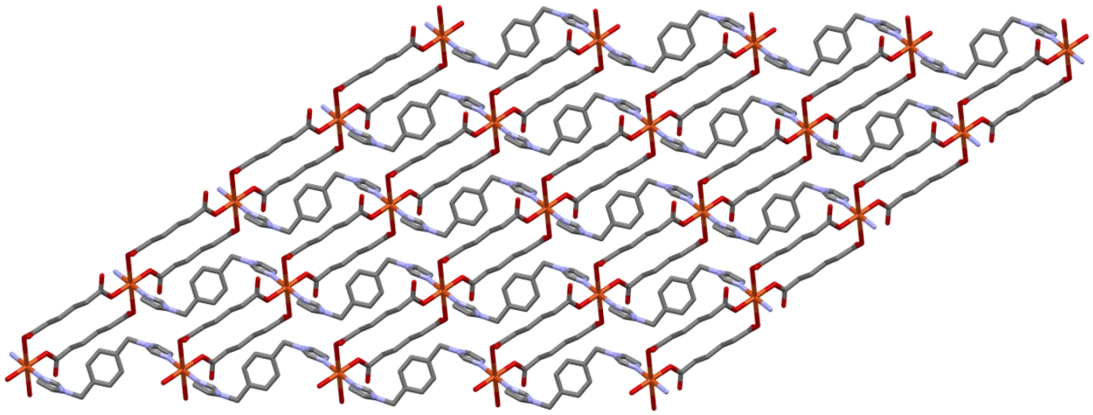

Fig. S2 View of 2D coordination network of **KA@CP-S3** along crystallographic "a" axis.

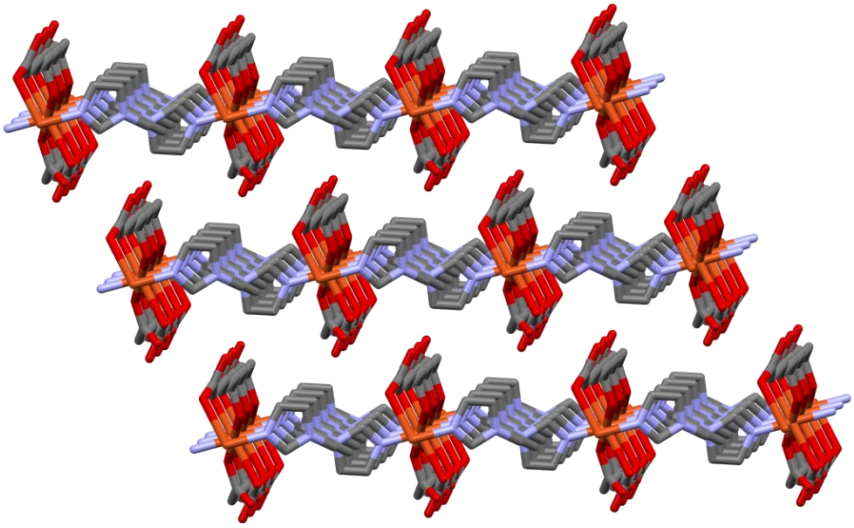

Fig. S3 View of 2D Parallel Layers of **KA@CP-S3** along crystallographic "c" axis.

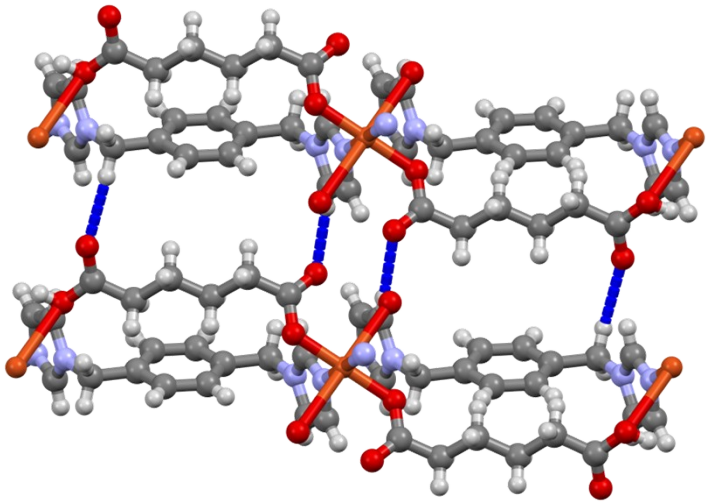

Fig. S4 View of C–H···O supramolecular hydrogen bonded 3D network of **KA@CP-S3** along crystallographic "b" axis.

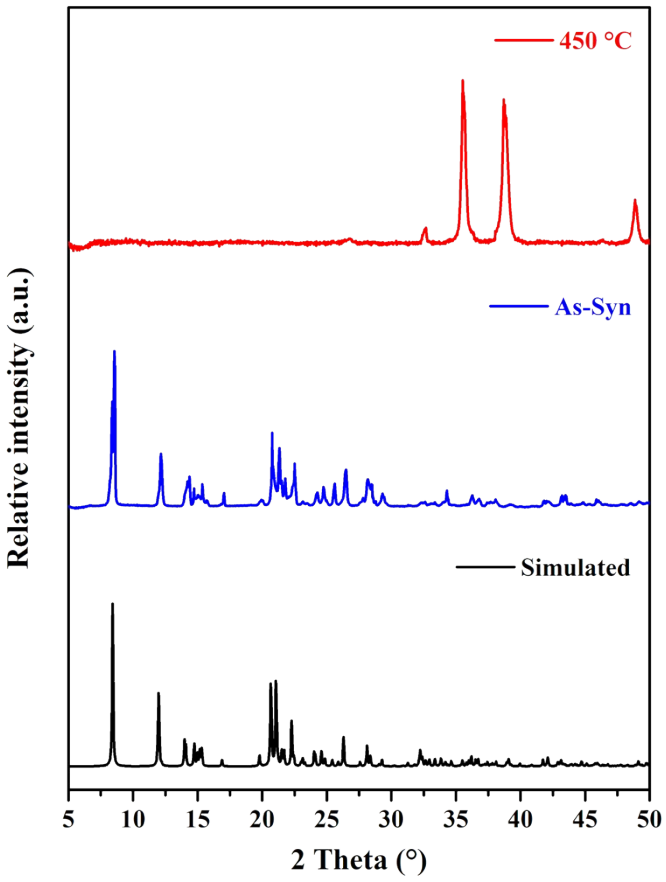

Fig. S5 Powder X-ray Diffraction spectra for **KA@CP-S3**.

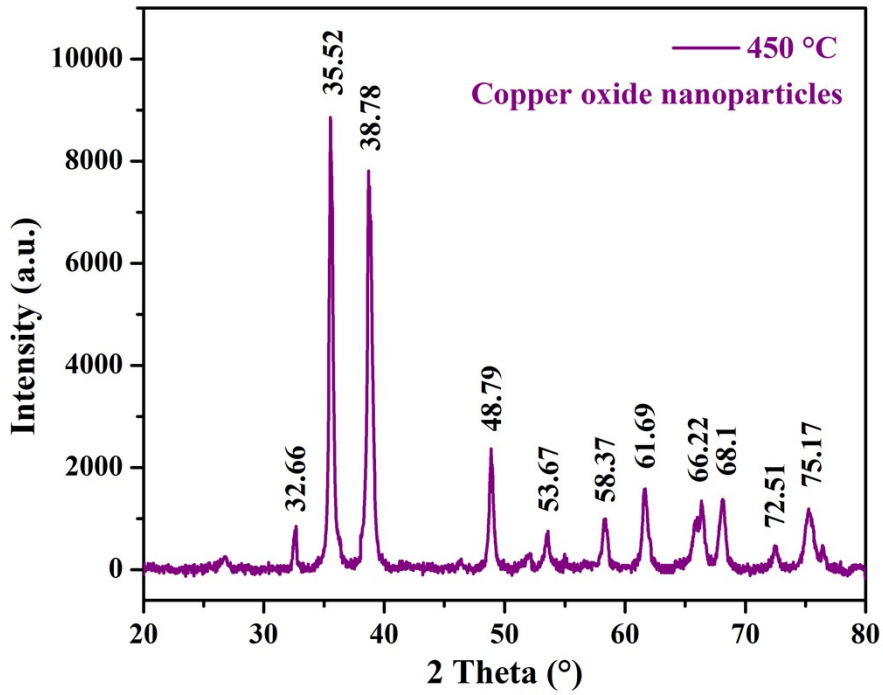

Fig. S6 PXRD patterns for CuO nanoparticles.

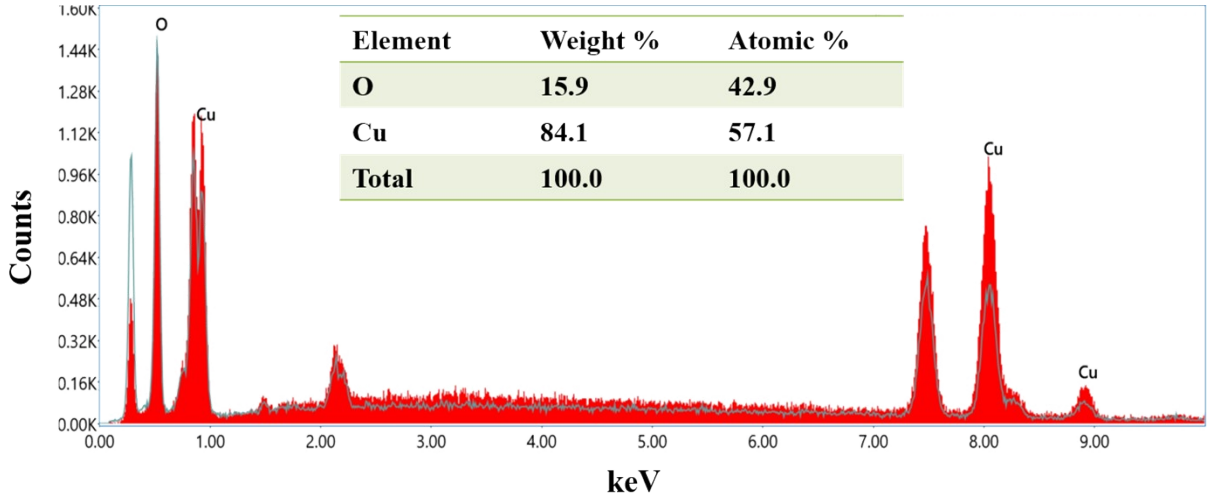

Fig. S7 EDAX diagram of CuO nanoparticles.

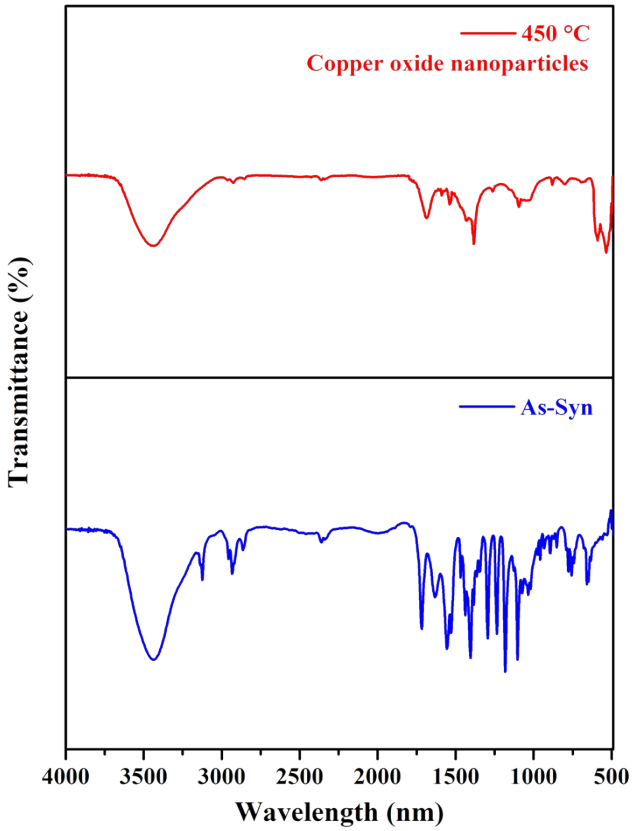

Fig. S8 FT-IR spectra for **KA@CP-S3**.

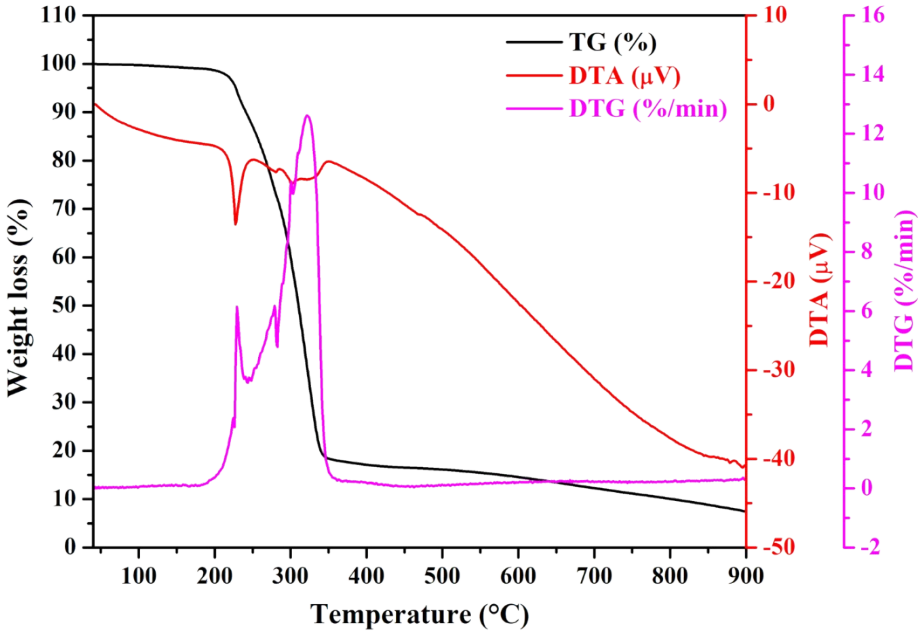

Fig. S9 TG-DTA-DTG curves for **KA@CP-S3**.

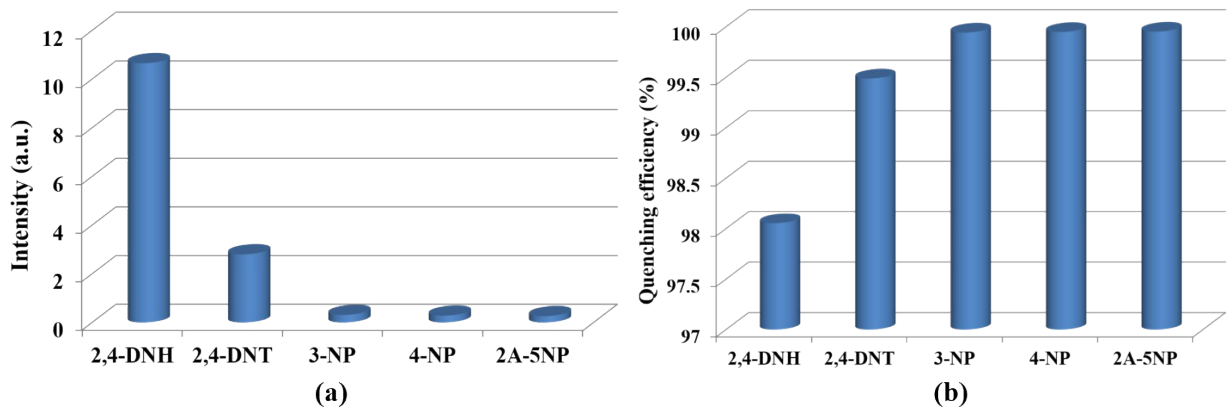

Fig. S10 (a) Fluorescence emission intensities and (b)Relative fluorescence quenching efficiencies of **KA@CP-S3** with different nitrobenzene derivatives.

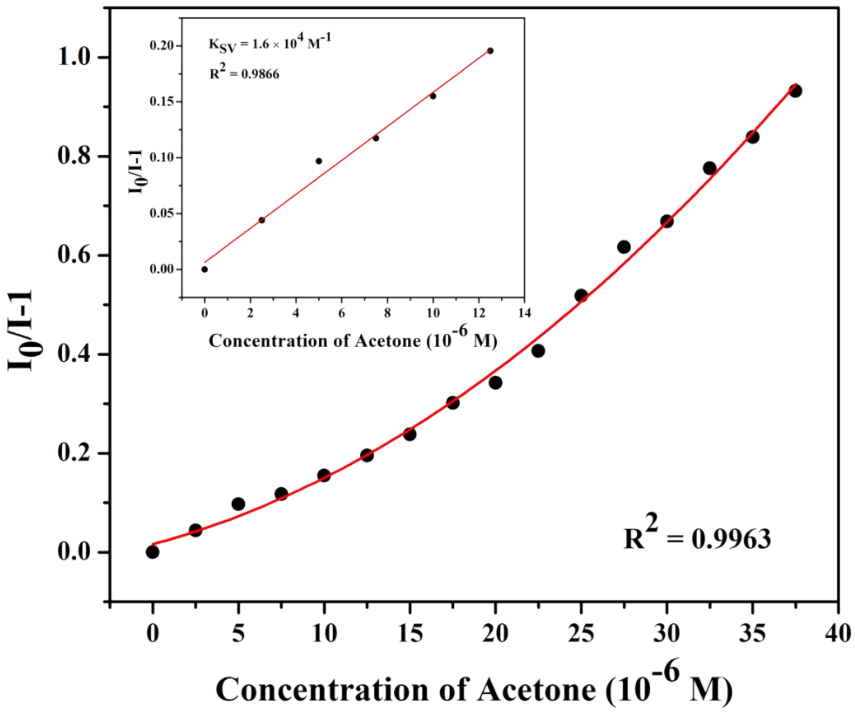

Fig. S11 *S–V* plot of **KA@CP-S3** dispersed in ethanolic solution after gradual addition of Acetone (1 mM), the linear *S–V* curve of **KA@CP-S3** at low concentration of Acetone (inset).

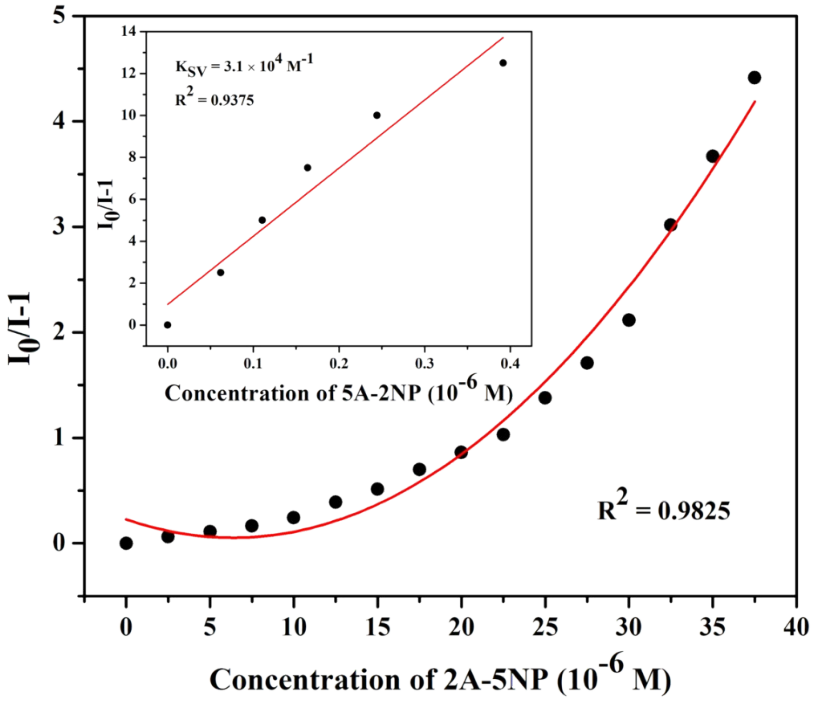

Fig. S12 *S–V* plot of **KA@CP-S3** dispersed in ethanolic solution after gradual addition of 2A-5NP (1 mM), the linear *S–V* curve of **KA@CP-S3** at low concentration of 2A-5NP (inset).

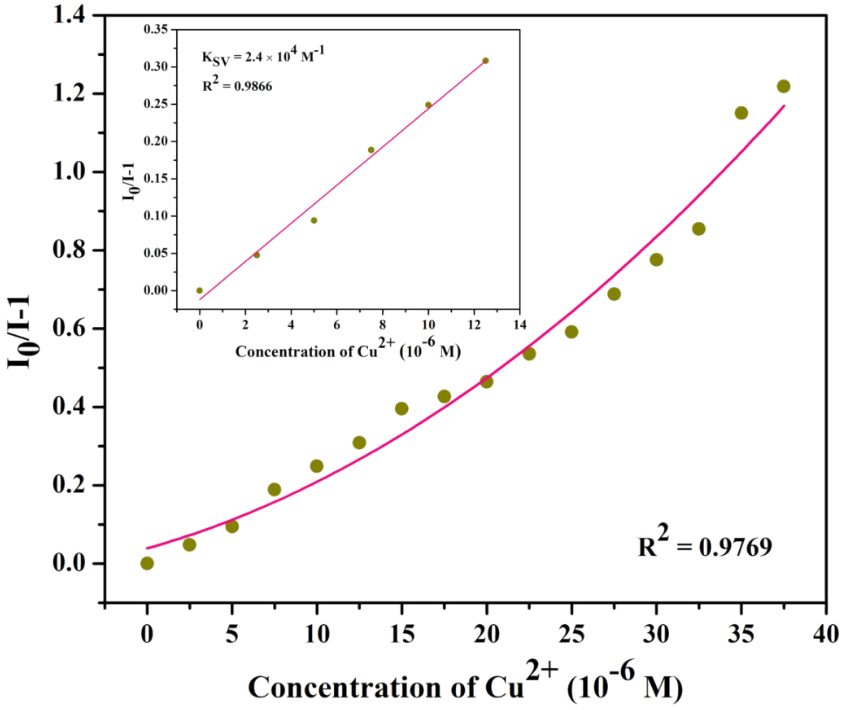

Fig. S13 *S–V* plot of **KA@CP-S3** dispersed in ethanolic solution after gradual addition of Cu^{2+} (1 mM), the linear *S–V* curve of **KA@CP-S3** at low concentration of Cu^{2+} (inset).

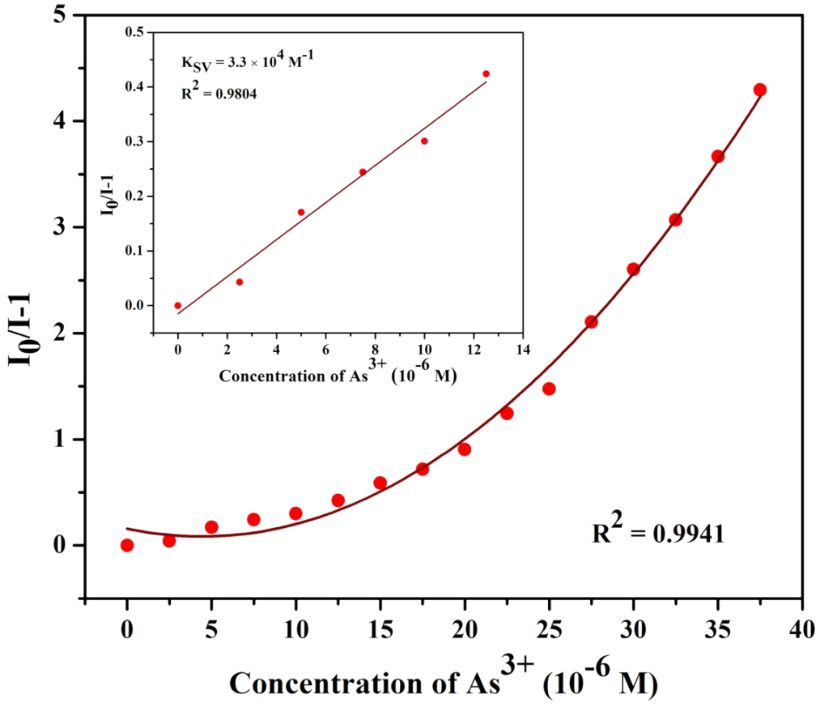

Fig. S14 *S–V* plot of **KA@CP-S3** dispersed in ethanolic solution after gradual addition of As^{3+} (1 mM), the linear *S–V* curve of **KA@CP-S3** at low concentration of As^{3+} (inset).

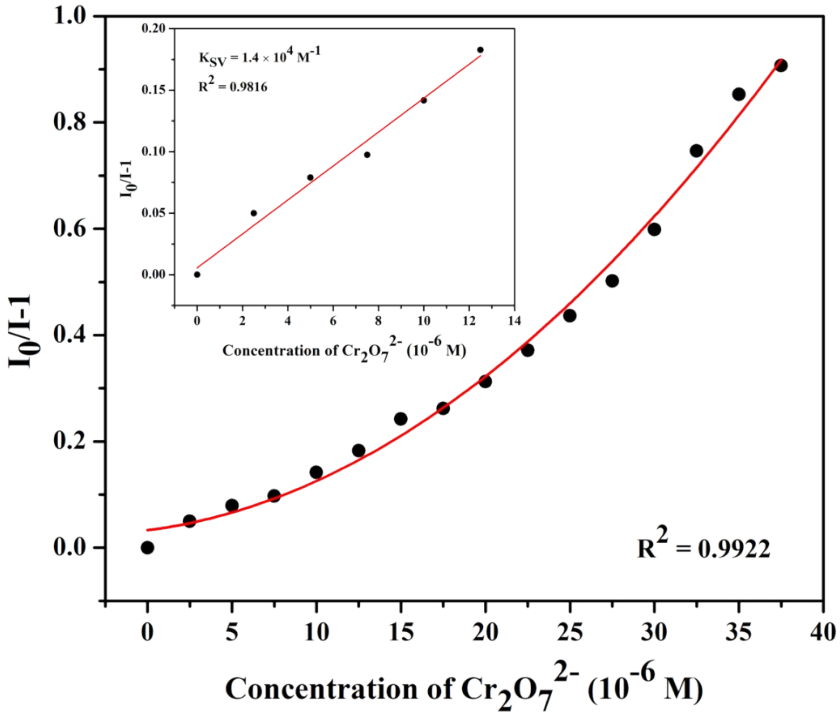

Fig. S15 *S–V* plot of **KA@CP-S3** dispersed in ethanolic solution after gradual addition of $Cr_2O_7^{2-}$ (1 mM), the linear *S–V* curve of **KA@CP-S3** at low concentration of $Cr_2O_7^{2-}$ (inset).

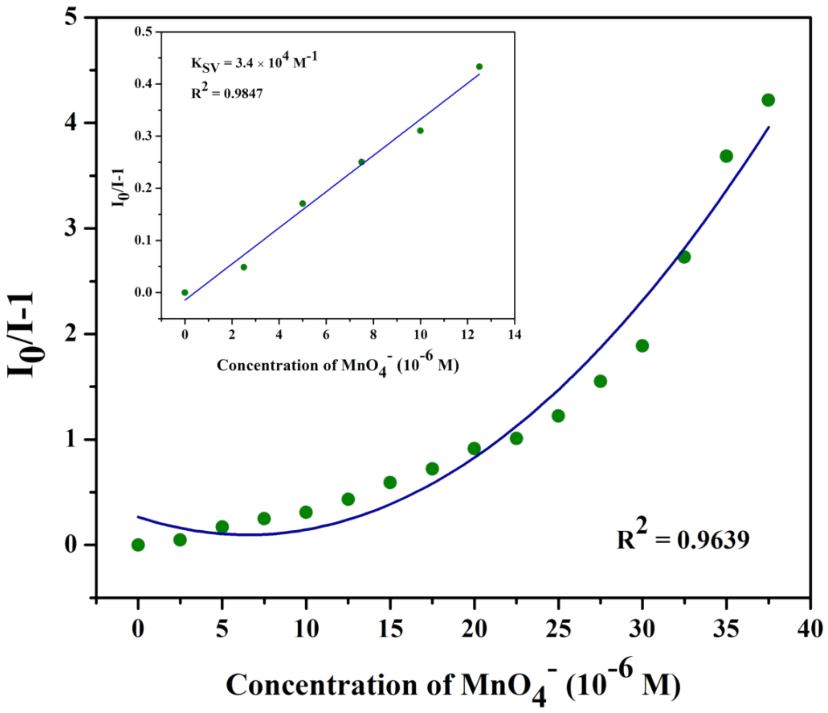

Fig. S16 *S–V* plot of **KA@CP-S3** dispersed in ethanolic solution after gradual addition of MnO_4^- (1 mM), the linear *S–V* curve of **KA@CP-S3** at low concentration of MnO_4^- (inset).

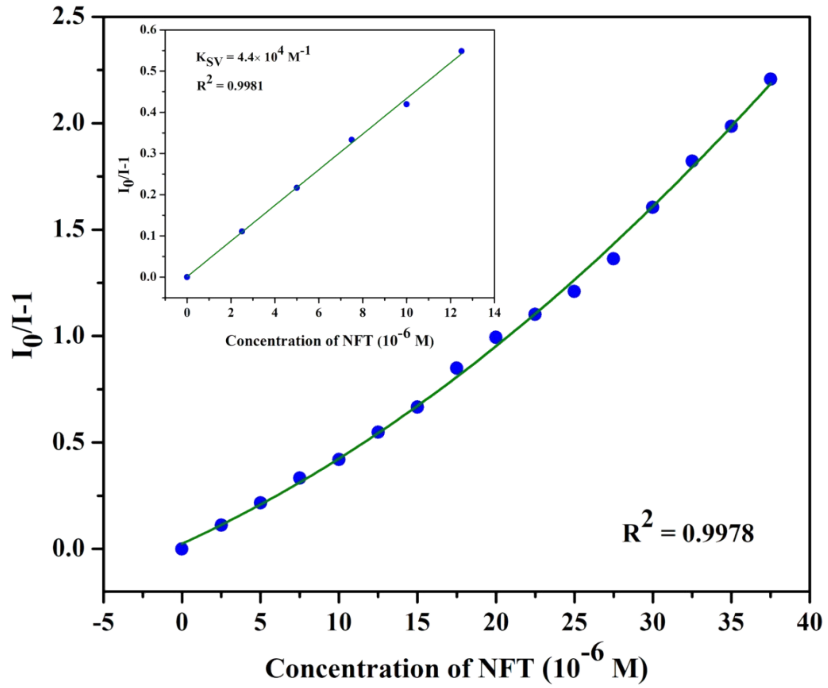

Fig. S17 *S–V* plot of **KA@CP-S3** dispersed in aqueous solution after gradual addition of NFT (1 mM), the linear *S–V* curve of **KA@CP-S3** at low concentration of NFT (inset).

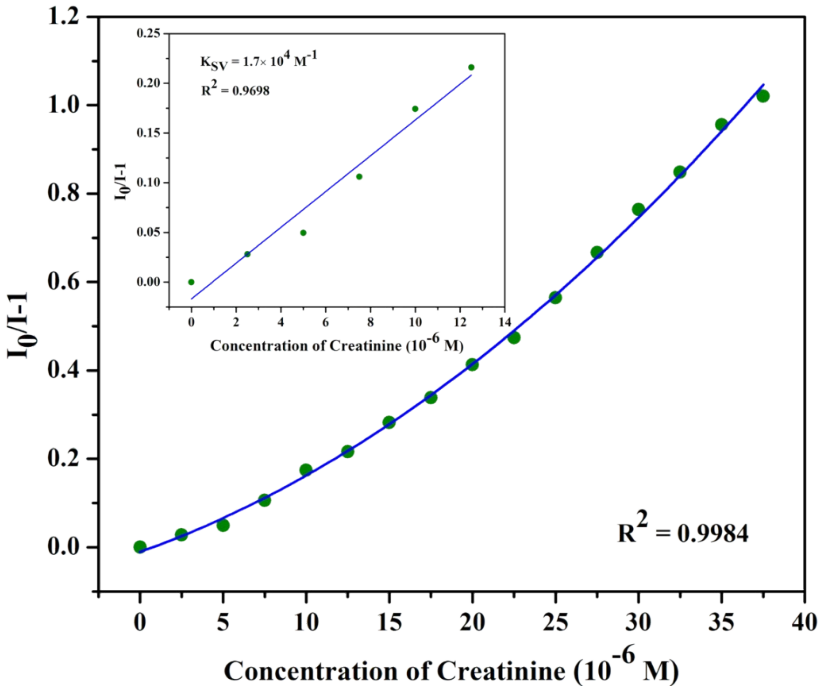

Fig. S18 *S–V* plot of **KA@CP-S3** dispersed in aqueous solution after gradual addition of Creatinine (1 mM), the linear *S–V* curve of **KA@CP-S3** at low concentration of Creatinine (inset).

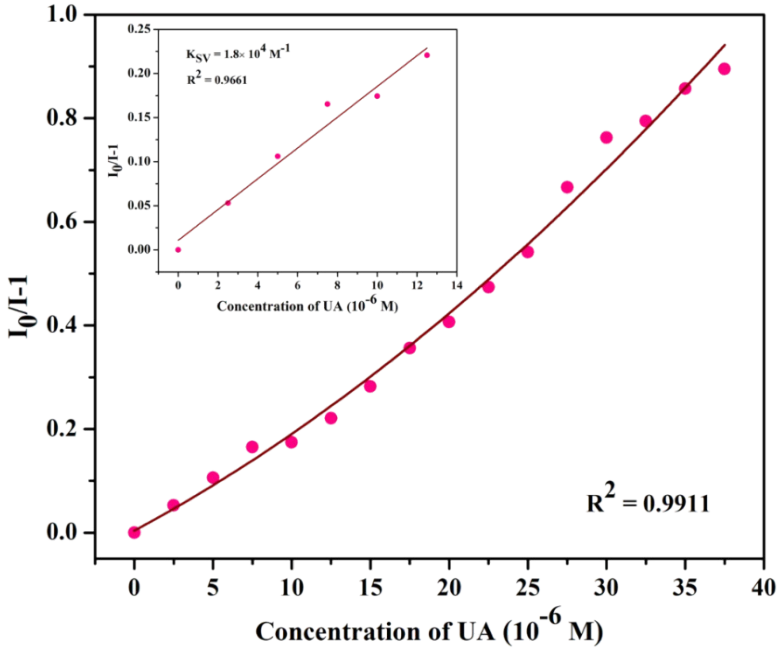

Fig. S19 *S–V* plot of **KA@CP-S3** dispersed in aqueous solution after gradual addition of UA (1 mM), the linear *S–V* curve of **KA@CP-S3** at low concentration of UA (inset).

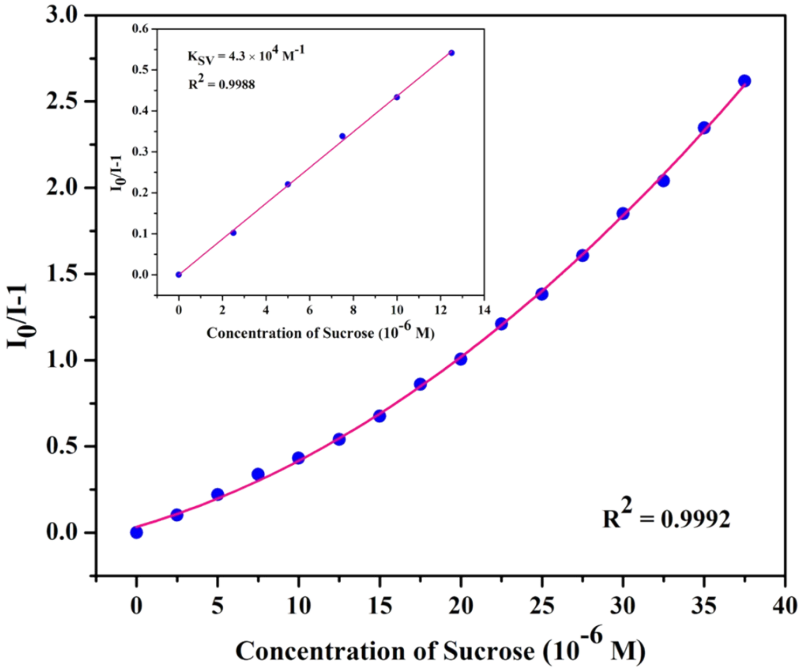

Fig. S20 *S–V* plot of **KA@CP-S3** dispersed in aqueous solution after gradual addition of Sucrose (1 mM), the linear *S–V* curve of **KA@CP-S3** at low concentration of Sucrose (inset).

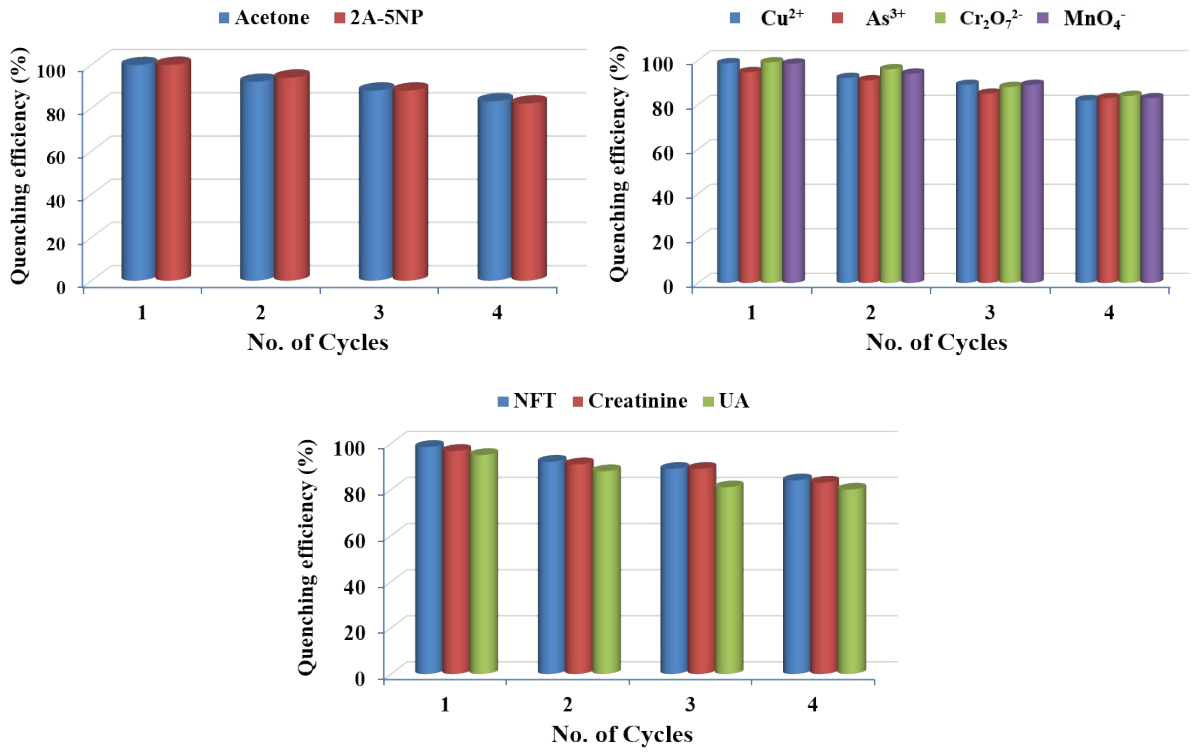

Fig. S21 Catalysts reusability of **KA@CP-S3** for each cycle.

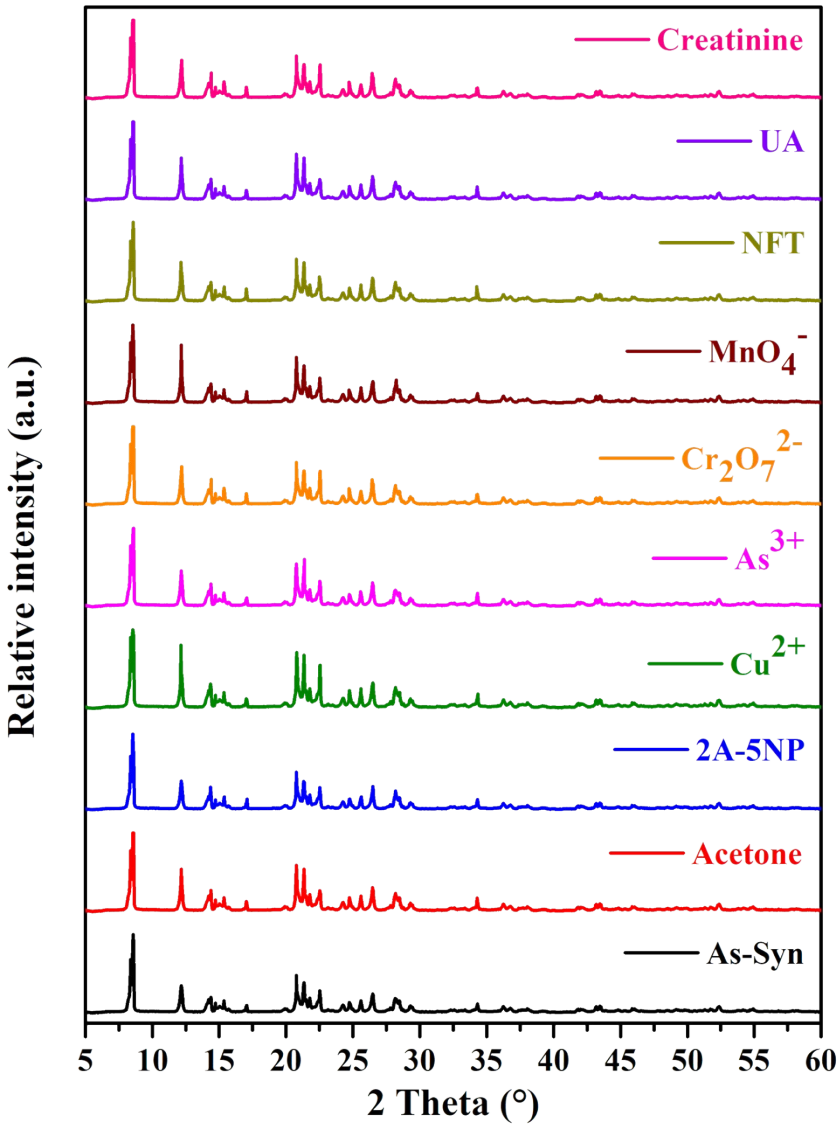

Fig. S22 PXRD patterns of **KA@CP-S3** before and after fluorescence sensing of various analytes.

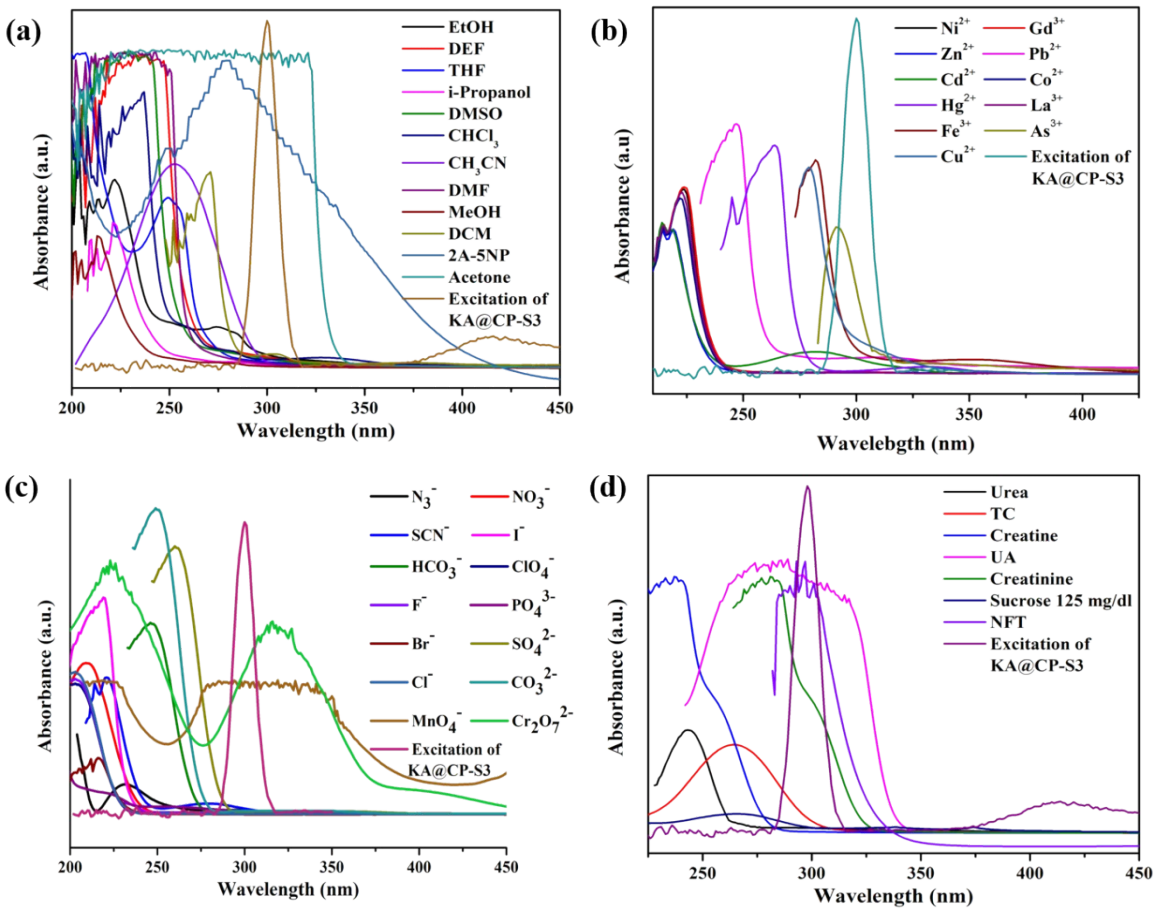

Fig. S23 Spectral overlap between the UV-Vis absorption spectra of various analytes and the excitation spectra of **KA@CP-S3**.

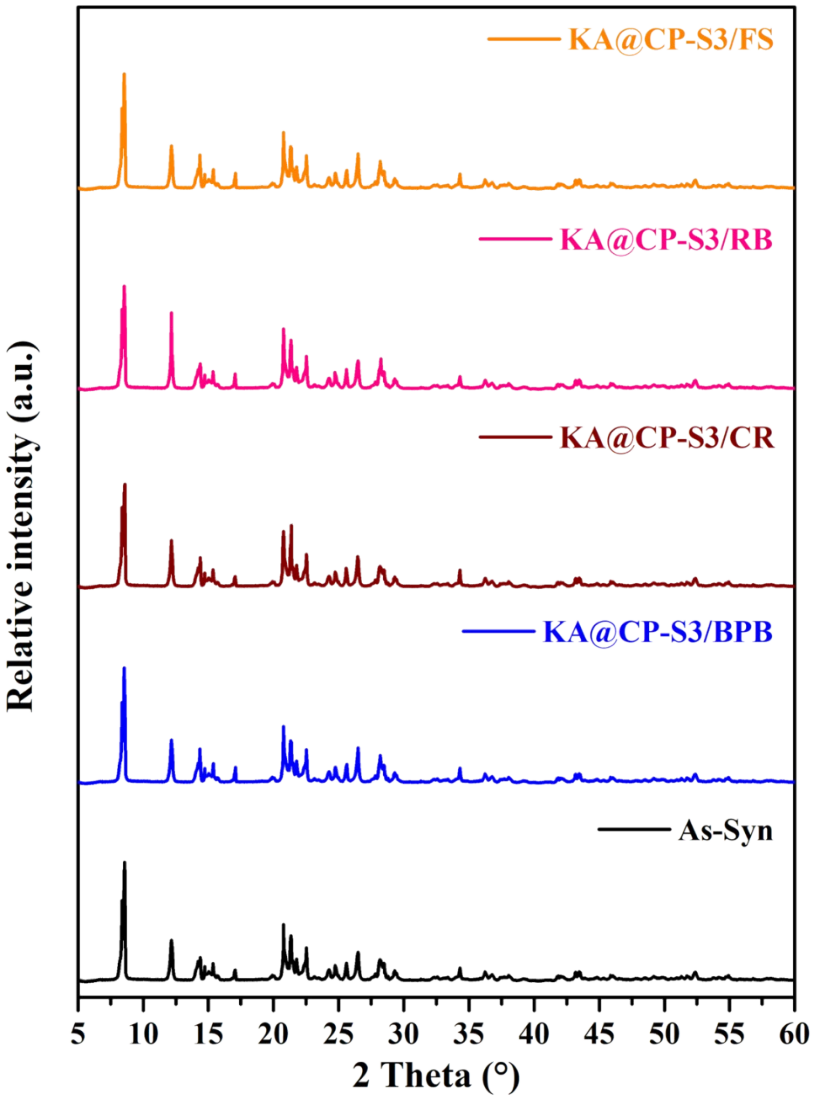

Fig. S24 PXRD patterns of **KA@CP-S3** before and after photocatalytic experiments with dyes (BPB, CR, RB and FS).

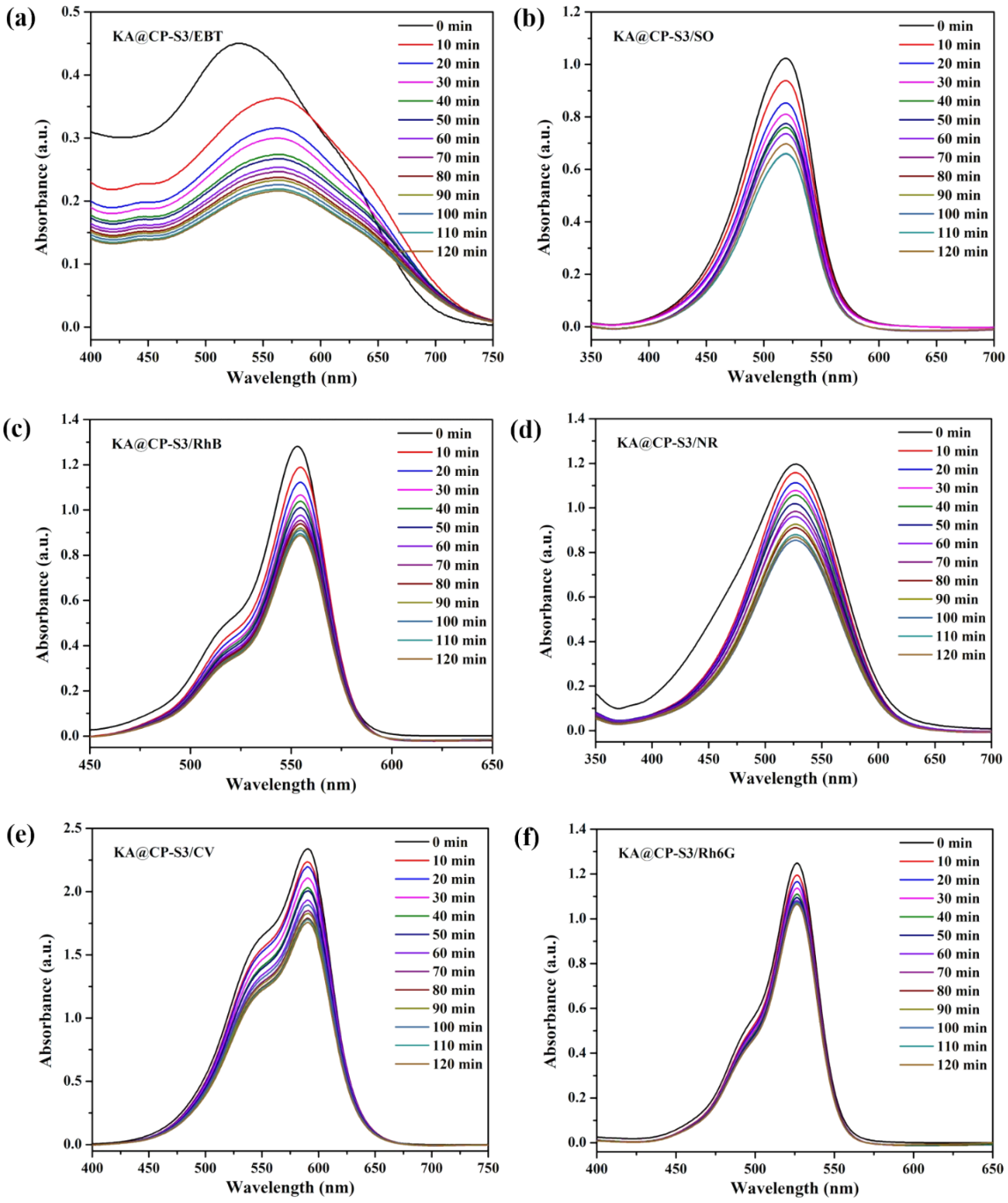

Fig. S25 Time-dependent UV-Vis absorption spectra of dyes (a) EBT, (b) SO, (c) RhB, (d) NR, (e) CV and (f) Rh6G with catalysts **KA@CP-S3**.

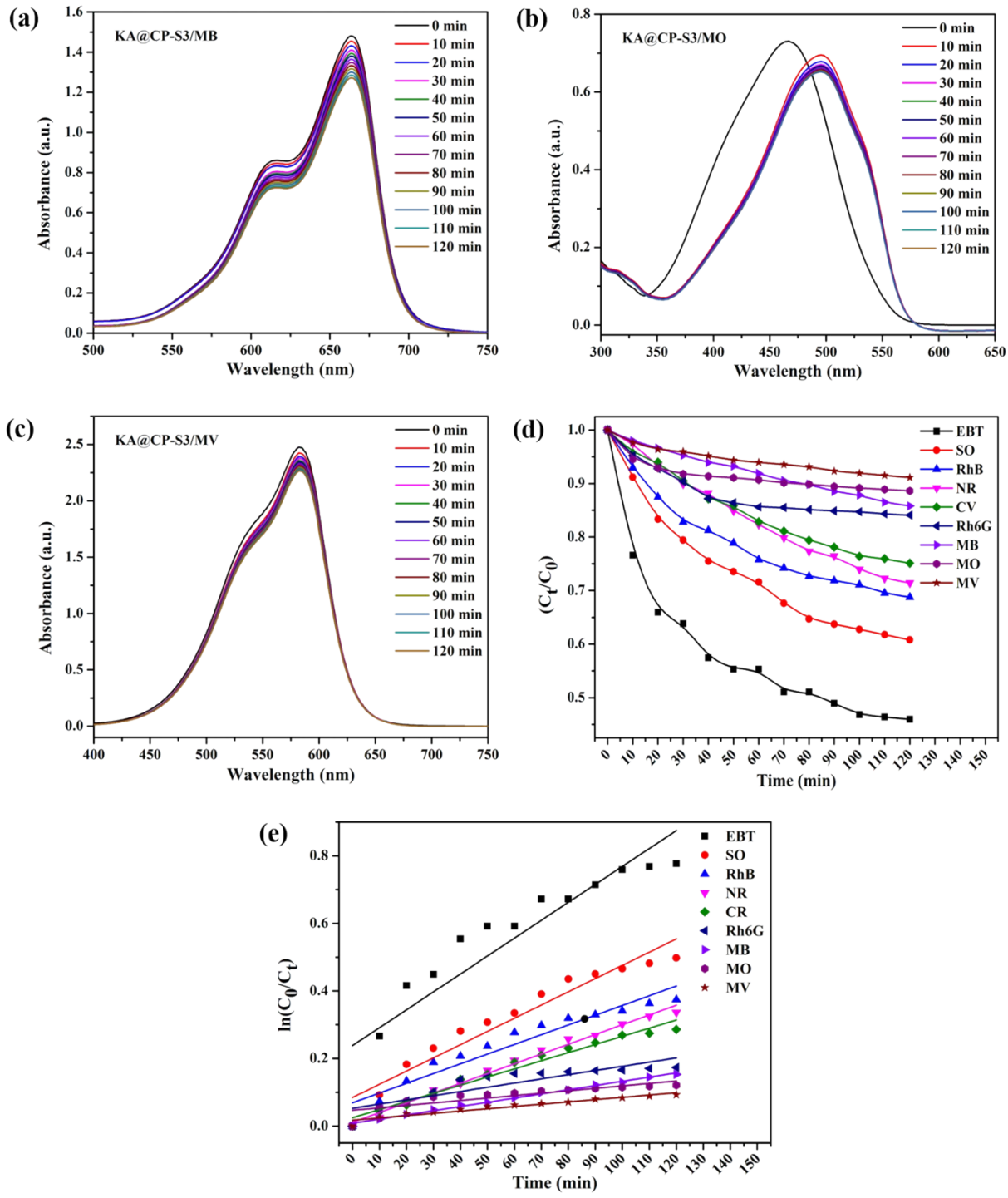

Fig. S26 Time-dependent UV-Vis absorption spectra of dyes (a) MB, (b) MO and (c) MV with catalysts **KA@CP-S3** (d) The Photocatalytic degradation kinetic plot of such dyes C_t/C_0 versus time interval plot and (e) Plot of $\ln(C_0/C_t)$ versus time interval in the presence of catalysts.

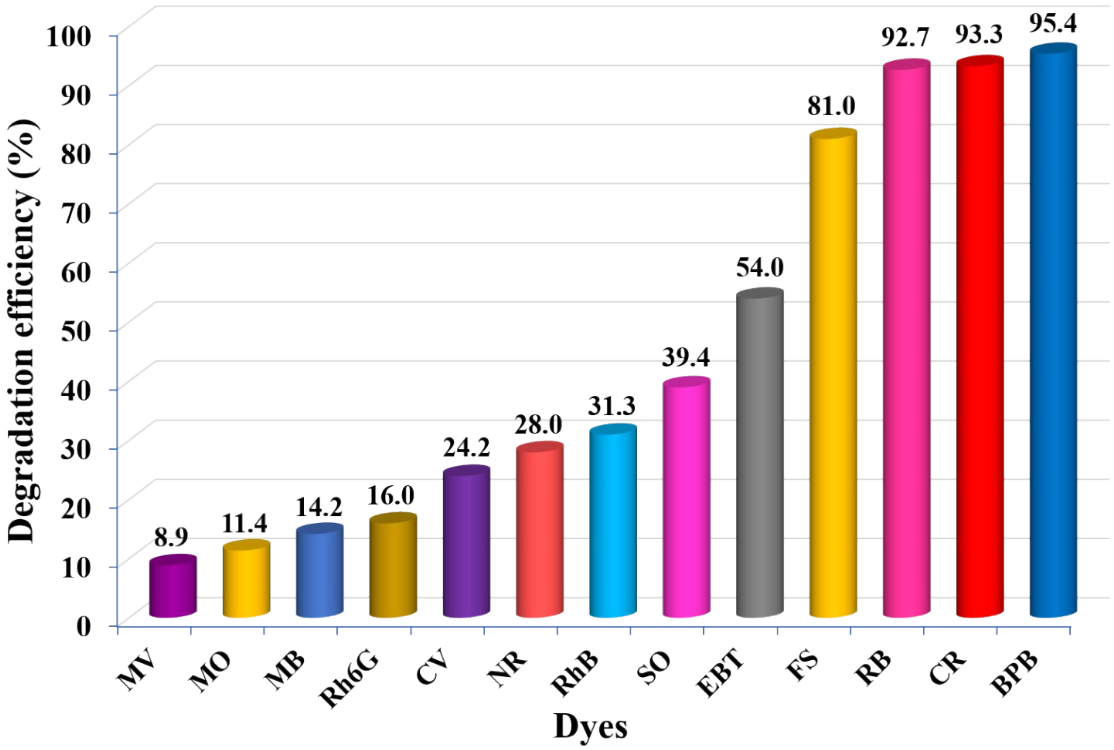

Fig. S27 Photocatalytic degradation efficiencies of **KA@CP-S3** for dyes.

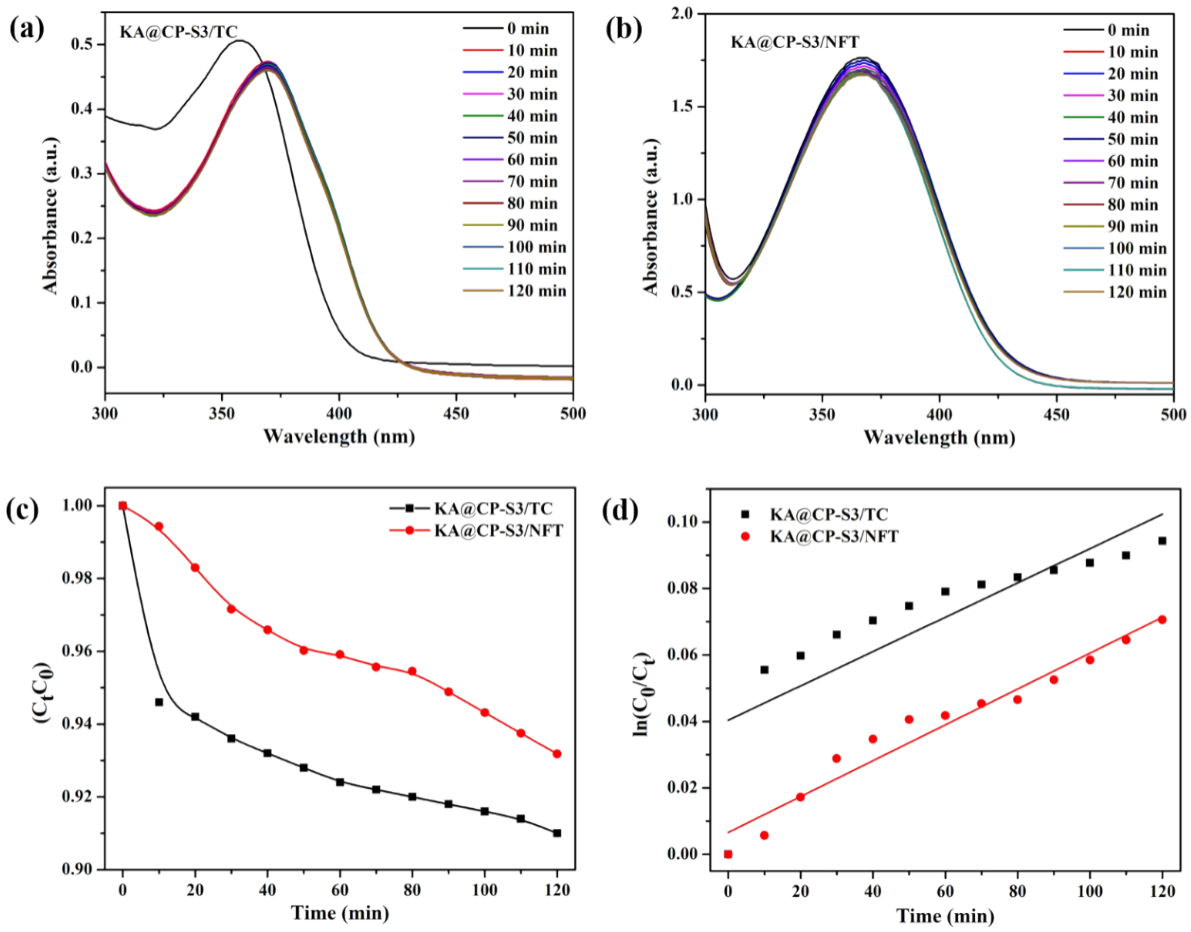

Fig. S28 Time-dependent UV-Vis absorption spectra of (a) TC and (c) NFT with catalysts **KA@CP-S3** (d) The Photocatalytic degradation kinetic plot C_t/C_0 versus time interval plot and (e) Plot of $\ln(C_0/C_t)$ versus time interval in the presence of catalysts.

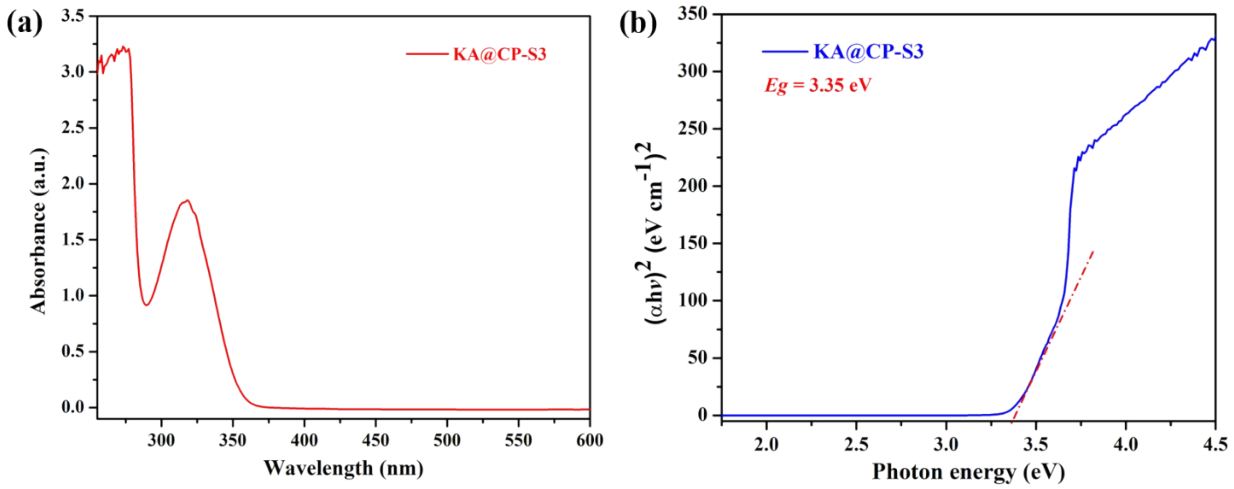

Fig. S29 (a) UV-Vis absorption spectra and (b) Tauc plot ($(\alpha h\nu)^2$ vs energy (eV)) for band gap study of **KA@CP-S3**.